Simulations of Heavy-Ion Fusion Using the TDHF Code: '*Sky3D*'

Edward Simmons

Department of Physics, University of Surrey,
Guildford, Surrey, GU2 7XH, UK

2014

Abstract

In this project, computational simulations of heavy-ion collisions are carried out using the TDHF code '*Sky3D*'. Two collision species are investigated (^{16}O - ^{16}O, and ^{20}O - ^{16}O), using two different Skyrme forces (SV-bas and SV-sym34). The fusion threshold energy, and fusion cross section are quantitatively investigated over both collision species, and also over the two Skyrme forces. The computational results for the fusion cross section are then compared to experimental data. Samples of output are shown, describing all four possible collision scenarios; fusion, deep inelastic collision, Coulomb repulsion, and peripheral collisions.

Contents

1. Heavy-Ion Collisions

1.1 Introduction to the Investigation

The basic premise of this project is to utilise a piece of Fortran90 code called '*Sky3D*', which has been written over many years by a number of contributors [1], to simulate the fusion of two heavy ions. The code accomplishes this by using a nuclear mean field model based on Skyrme forces, by first calculating a static ground state and then completing a dynamic, forward integration in a 3D Cartesian mesh [1]. By varying a number of input variables and initial conditions, many different investigations may be carried out using *Sky3D*.

There are two distinct collisions that will be simulated: ^{16}O - ^{16}O, and ^{20}O - ^{16}O. The investigation to be carried out is as to what affect the addition of neutral matter in the second collision has on both the cross section of the reaction, and the energy/ angular momentum spectra across which successful fusion is possible. Also to be investigated is how changing the mathematical model of the nuclear strong force affects both the reaction cross section and the successful fusion threshold.

1.2 Basic Interactions

The interaction of two heavy ions is a complex process. Nuclei themselves are intricate and complicated structures, comprising of many nucleons, potentially carrying relatively large angular momenta, and possibly in any manner of excited state. Throughout this report, I will refer to the total energy of the system as the centre of mass energy, E_{cm}, which is analogous to the effective kinetic energy of the colliding nuclei, i.e. higher centre of mass energies correspond to higher kinetic energies.

At low energies, the two nuclei will only experience a Coulomb interaction, which is proportional to their charge (i.e. proton number), given by:

$$|F_C| = \frac{|Z_1 Z_2 e|}{4\pi\varepsilon_0 r^2} \tag{1}$$

Where Z_1 and Z_2 are the respective proton numbers of the colliding nuclei, e is the elementary charge, ε_0 is the permittivity of free space, and r is the separation between the two nuclei. This interaction can either take place as an elastic collision, meaning that momentum is completely conserved across the event [2], or as an inelastic collision where there is some Coulomb excitation in the nuclei [2]. This is shown diagrammatically in fig. 3 as the yellow line. No other type of interaction will occur unless the centre of mass energy is high enough to overcome this repulsive force. The nuclei must overcome a 'Coulomb barrier', shown in fig. 1, the height of which climbs rapidly as the nuclei move closer to one another, due to the inverse-square nature of the force.

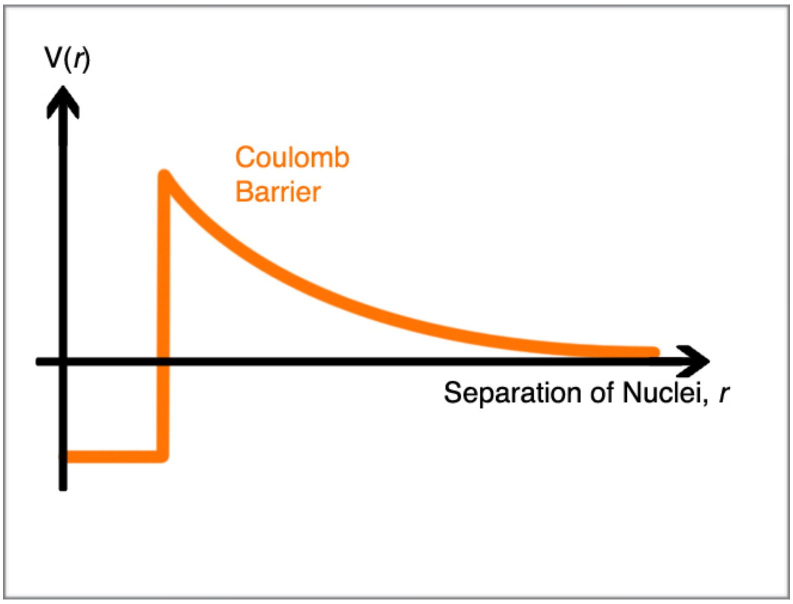

Figure 1 *The Coulomb Barrier*

As the distance separating two charged objects increases, the electric potential between them falls off at a ratio of *1/r*. In order for two nuclei to fuse, they must overcome this energy barrier to reach a separation low enough for the nuclear strong force to act upon the nucleons,

The other determining factor as to what type of interaction will occur is referred to as the impact parameter, *b*, which is defined as the perpendicular distance to the closest approach if the projectile were undeflected [3]. The impact parameter corresponds to an orbital angular momentum, *l*, which may be expressed via the relation [4]:

$$l = b\sqrt{2\mu E_{cm}} \tag{2}$$

Where μ is the reduced mass of the system. In these simulations, *b* is measured in units of femtometres [fm], and is on the order of 0-10fm. Across this range, along with a range of E_{cm} values, there are four possible nuclear interaction scenarios; incomplete fusion (otherwise known as deep inelastic collision), fusion, a peripheral collision, or the aforementioned elastic scattering [2].

Deep inelastic collision, or incomplete fusion, occurs when the overlap region of the two colliding nuclei is relatively low, but still sufficient enough for strong interactions to occur, i.e. at higher impact parameters (shown in fig. 3 as the green line) [2]. In these reactions, a significant proportion of the kinetic energy of the ions is converted into internal excitations in the nuclei [2]. In a deep inelastic collision, the two colliding nuclei temporarily form a dinuclear system which is connected by a 'neck', along which energy, and nucleons, may be transferred [2]. For the purposes of this work, the connecting neck is one of the most import an features of the system, as it is the feature by which the program determines whether or not the two nuclei are currently fused as one. After some time has passed - the length of time being dependant on the initial conditions of the collision - the dinuclear system will disintegrate and the two nuclei will be separated, although they may not necessarily be the same nuclei that entered the system due to nucleon exchange.

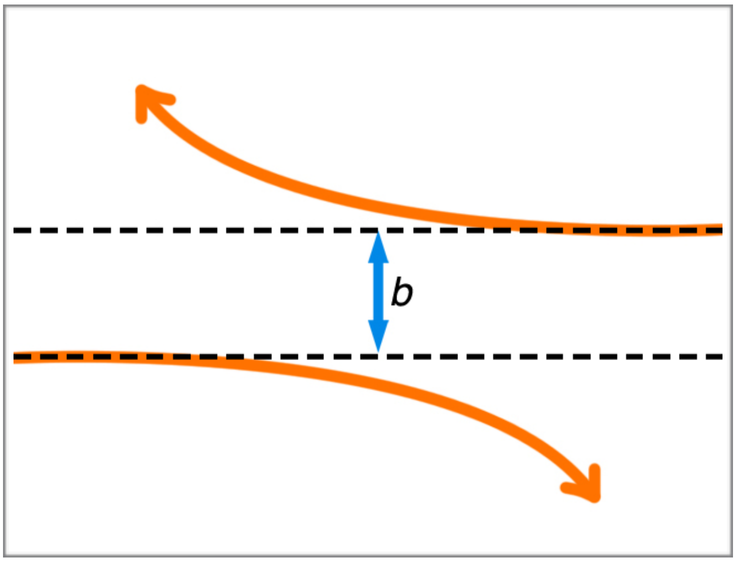

Figure 2 *Diagram of the impact parameter, b*

This is a simple graphical representation of what is meant by the perpendicular distance of closest approach. Any two colliding nuclei will repel one another, so the impact parameter is taken as the perpendicular distance between their respective initial velocity vectors.

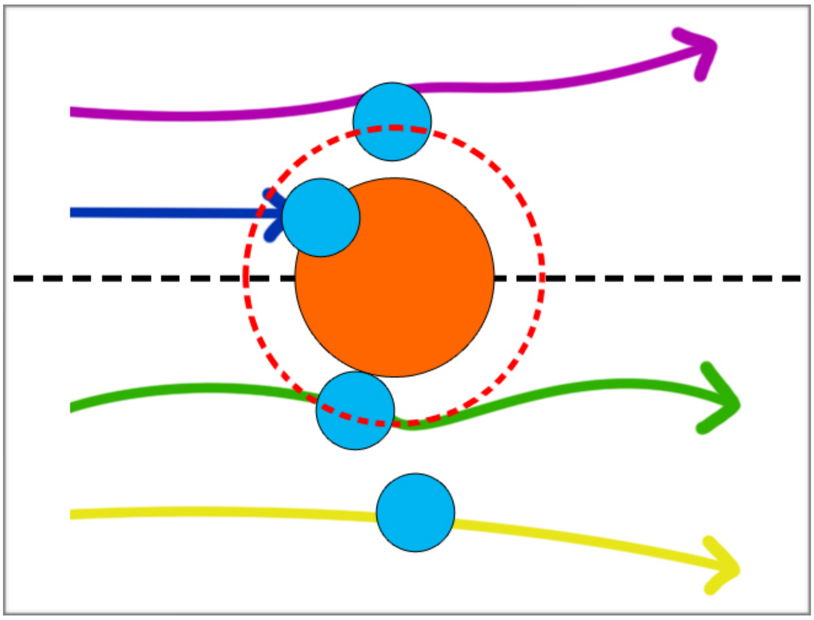

Figure 3 *Nuclear Interaction Scenarios*

Shown here are the 4 possible interaction types for two colliding nuclei. From top to bottom: a peripheral collision, a fusion reaction, and incomplete fusion reaction (or deep inelastic collision), and a coulomb repulsion. The red dotted line indicates a critical distance from the target nucleus that determines which type of interaction takes place, and is a consequence of the Coulombic force of repulsion between the two colliding nuclei.

A peripheral collision (shown in fig. 3 as the purple line) also occurs at higher impact parameters, and is described as when the two nuclei brush past each other, possibly exchanging some nucleons, but not forming a dinuclear system [2].

Fusion (shown in fig. 3 as the blue line) is where the two-ion interaction leads to the production of a single, composite nucleus, which initially will be very far from statistical equilibrium - much of the composite system's excitation energy is in the form of an orderly collective translational motion of the nucleons within the nucleus [2]. Over time, through collisions, nucleon-nucleon interactions, and thermalisation, the compound nucleus will reach a statistical equilibrium [2].

1.3 Fusion Cross Sections

The fusion reaction cross section may be expressed by the relation [3]:

$$\sigma_f = \frac{\pi\hbar^2}{2\mu E_{cm}}\left[(l_{upper}+1)^2-(l_{lower}+1)^2\right] \tag{3}$$

Where l_{upper} and l_{lower} are the upper and lower limits of the angular momenta where fusion is possible, obtained via applying eq. (2) to my results. It was necessary to reduce this relation to more convenient units via:

$$\sigma_f = \frac{\pi(\hbar c)^2}{2\mu c^2 E_{cm}}\left[(l_{upper}+1)^2-(l_{lower}+1)^2\right] \tag{4}$$

Where $\hbar c$ = 197.3 MeV·fm, and μc^2 is the mass-energy of the system. This reduction in units allows E_{cm} to be expressed in units of MeV, and the cross section therefore will be in units of fm^2.

Traditionally, in TDHF calculations of fusion cross section, a reaction is deemed a successful fusion it the composite body undergoes one full rotation without disintegrating [3]. This composite body is then assumed to have lost most of the memory of its entrance channel, and will eventually reach a thermally stable state [3]. This purely qualitative approach is ineffective when attempting to run a fully automised, self-sufficient program (the modifications made to rectify this problem are discussed in chapter 2).

1.4 Mean Field Theory & the Hartree-Fock Equations

The use of mean field theory is primarily aimed at gaining a microscopic, quantum-mechanical understanding of matter [4]. The basic premise is that a complex collection of nucleon-nucleon reactions can be treated through averaging those interactions in the form of a one-body density matrix [4]. The Honenberg-Kohn theorem states that knowledge of these densities (which are obtained from the many-body system's hamiltonian) means that one has knowledge of the entire system, and it's ground state observables [4] [7].

This averaging of these nucleon-nucleon interactions creates what is known as a mean field. All the nucleons being considered are fermions, so they must therefore obey the

Pauli exclusion principle, which states that no two fermions may occupy the same quantum mechanical state simultaneously [8]. Due to this principle, most collisions in the interior of the nucleus are Pauli-blocked, causing the nucleons' mean free path to be much longer than the average interaction distance, which is ~1fm [9]. Therefore, the nucleons may be described, to a first approximation, as interaction-free particles moving in a mean-field created by all the other particles [9]. Hence, the wavefunction of this collective state must be anti-symmetric under the exchange of coordinates between any two nucleons [4].

This leads to the ground-state of any nucleus being written as an anti-symmetrical product of occupied states, otherwise known as a Slater determinant, which comprises of a complete set of orthonormal wavefunctions [4]. This set of wavefunctions is the basis for the Hartree-Fock approach, which was developed by P. A. M. Dirac in 1930 [10].

The thought process behind Hartree-Fock theory is to start with the hamiltonian of the many body system [4]:

$$\hat{H} = \sum_{i=1}^{A} \frac{\hat{p}_i^2}{2m_i} + \frac{1}{2}\sum_{i \neq j}^{A} V(r_i, r_j) \tag{5.1}$$

Where *A* is the mass number of the nucleus in question. The potential term contains all the components of the nucleon-nucleon force, including any Coulombic interaction [4]. The mean-field approach to this problem then is to express said potential as a one-body, mean-field [4]. From this, a simplified solution for the Hartee-Fock equations may be formed [4]:

$$\varepsilon_i \phi_i(r) = -\frac{\hbar^2}{2m}\nabla^2 \phi_i(r) + U_H^{(i)}(r)\,\phi_i(r) - \int U_F^{(i)}(r, r')\,\phi_i(r')\,dr' \tag{5.2}$$

This gives the single particle energies, as calculated from the one-body Schrödinger equation [4]. The second term in (5.2) is the direct term, or the 'Hartree' term, and is dependant only upon the one-body density [4]:

$$U_H^{(i)}(r) = \sum_{j>i}^{A} \int \phi_j^*(r')\,V(r, r')\,\phi_j(r')\,dr' \tag{5.3}$$

The third term in (5.2) is the exchange, or 'Fock' term, and is a result of the antisymmetrisation of the many-body wavefunction [4]:

$$U_F^{(i)}(r, r') = \sum_{j>i}^{A} \phi_j^*(r')\,V(r, r')\,\phi_j(r') \tag{5.4}$$

The solutions to (5.2) form a set of single-particle wavefunctions that form the ground-state basis of the Slater determinant, i.e. a one-body density matrix [4]. Since the solution depends on the wavefunctions that are being solved for (the potential terms), it is non-linear, and therefore must be solved through an iterative solution [4]. This means starting with a set of trial wavefunctions, hence the need for a static run of the program before a dynamic integration may take place.

1.5 The Skyrme Force

Otherwise referred to as the Skyrme energy functional, the Skyrme force models the effective interaction between nucleons [11]. The basis of the Skyrme force was developed from the idea that the energy functional could be expressed in terms of a zero-range expansion, which led into the derivation of the simplified Hartree-Fock equations, i.e. eq. (5.2) [4]. By making this approximation, the number of iterations required to complete a computational integration of a complete set of wavefunctions was greatly reduced [4]. In this model, the total binding energy of the system is given as the sum of the kinetic energy, the Coulomb energy, and the Skyrme energy functional [4]:

$$E = E_{Kinetic} + E_{Coulomb} + \int \varepsilon_{Skyrme} dr \tag{6}$$

This Skyrme force can be calibrated through a set of eight parameters ($x_0, x_1, x_2, x_3, t_0, t_1, t_2, t_3$) to fit experimental data, and herein lies the ultimate flaw with using the Skyrme energy functional to model nucleon-nucleon interaction (i.e. the nuclear strong force). The experimental data used for these parameters varies greatly, and as a result there are many different versions of the Skyrme force that have been put forward by researchers. This creates the problem of choosing an appropriate model Skyrme force to work with.

2. Processing Output

2.1 Qualitative and Quantitative Methods

The primary output of this investigation was a series of .png files that were generated via gnuplot script. These .png files were compiled into an animated .gif file by the terminal. These animations were the primary means by which results could be analysed qualitatively, i.e. looking to see whether or not the two nuclei had fused at the end of the dynamic integration. However, it became apparent that if the process was to be fully automated (by which I mean self-analysing), a quantitative method of determining whether or not the two colliding nuclei had fused was required. It became necessary at this point to gain some understanding of how the individual modules of the program worked, which was provided by *The TDHF Code: Sky3D* [1]. The modules that needed to be to modified/ investigated were *'Dynamic'* and *'Twobody'* respectively.

The role of *'Twobody'* is to analyse the the initial and final stages of the heavy-ion collision. It evaluates whether or not the two nuclei are separate bodies by calculating the density along the line that connects their centres of mass. This line is given by the module *'Moment'*, which calculates the complete Cartesian quadrupole tensor [1]. *'Twobody'* contains within it a variable named *'istwobody'* which is a logical variable. If, when the quadrupole tensor is integrated along, there is an area of sufficiently low density, the variable *'istwobody'* is deemed true, i.e. the two nuclei are separate. So, therefore, if at the end of a dynamic integration using *Sky3D*, the current value of *'istwobody'* is true, then there was not a successful fusion. Likewise, if *'istwobody'* was false, then there must have been a successful fusion.

Therefore, in order to quantitatively evaluate whether or not there had been a successful fusion, it was necessary extract the *'istwobody'* variable from it's respective module, and use it as a flag (i.e. a criteria upon which the need to write to an output file is determined).

To do this, the module *'Dynamic'* was modified, which is the module responsible for the successful propagation of the system [1]. Essentially, output is only written if it is the final iteration of the program, or if the two nuclei have moved beyond the grid spacing, which is also an exit criteria for the entire program (the program will stop running if the nuclei exit the grid). This output could then be plotted as a 3D heat map in gnuplot, showing the energy/ angular momentum boundary between successful and unsuccessful fusion.

It was necessary to make this modification in *'Dynamic'* specifically because there is an order in which the modules are called. Much like a chain of dominoes, the modules of *Sky3D* depend on each other in a cascading fashion. *'Dynamic'* was able to call upon *'Twobody'* and was therefore ideal. The very nature of *'Dynamic'* was also ideal for this modification, because it was already responsible for writing output to the screen, and had the appropriate parallelisation structure in place (i.e. ensuring only one of the many processors carried out the responsibility of writing the output file).

Classically, and experimentally, a fusion reaction is deemed successful if the coalesced body undergoes one or more complete rotations as a composite system, without disintegrating [5] [6]. The experimental data that is used to compare with this computationally gained data will be based upon that assumption.

3. Density/ Time Animations

3.1 Examples of Output: The Four Reaction Scenarios

As mentioned previously, with the combined effort of the main program and some shell scripts, the primary output of this investigation was a series of images that could be sequenced as an animation. The program would generate output data every 25 iterations

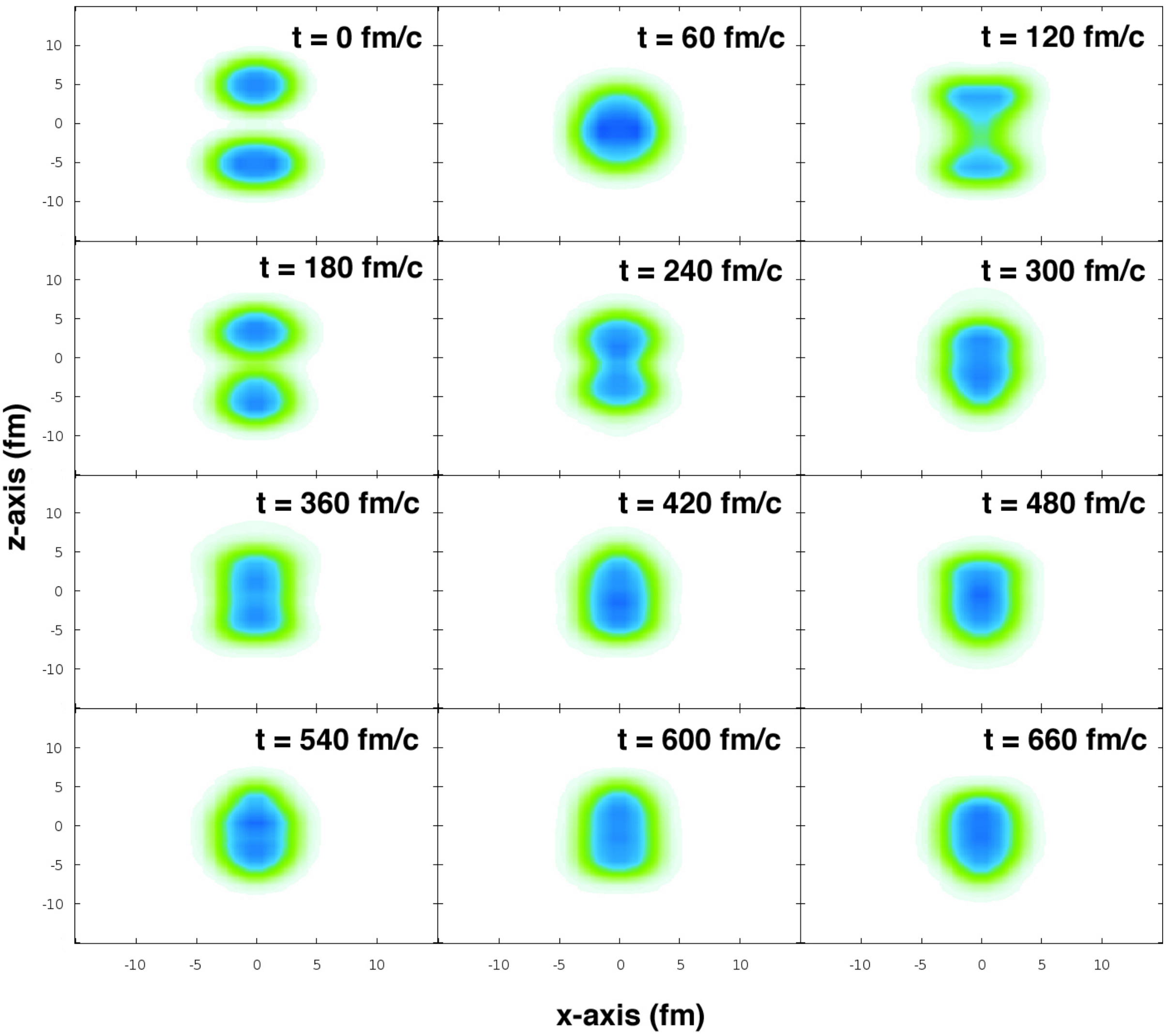

Figure 4 *Example of a Fusion Reaction: ^{20}O - ^{16}O*

Here we have an ^{20}O nucleus colliding with an ^{16}O nucleus, under the Skyrme force SV-sym34. The impact parameter, b = 0 fm, and the centre of mass energy, E_{cm} = 94 MeV. This collision is close to the fusion/ no fusion border, which means that there are many internal excitations, and it takes the system a long time to relax into a state of thermal equilibrium. This is but a small sample of all the frames that were generated. A high number of frames was required for greater clarity in the animations. For a full, 3600 iteration simulation like this one, there would have been 144 frames generated, resulting in an ~14s animation.

(equivalent to a time step of 5 fm/c) up to a maximum of the 3600th iteration. This number was chosen based on early observations made on how many iterations were required for a composite system to make a full rotation, similar to the experimental success criteria just mentioned. In many cases however, the full 3600 iterations were not required as the nuclei would exit the designated grid spacing, causing the program to cease.

In all of these examples, density is represented by colour; denser areas correspond to darker colours. This was an incredibly useful tool in observing how energy, and nuclear matter, was transferred and exchanged between the two halves of the system.

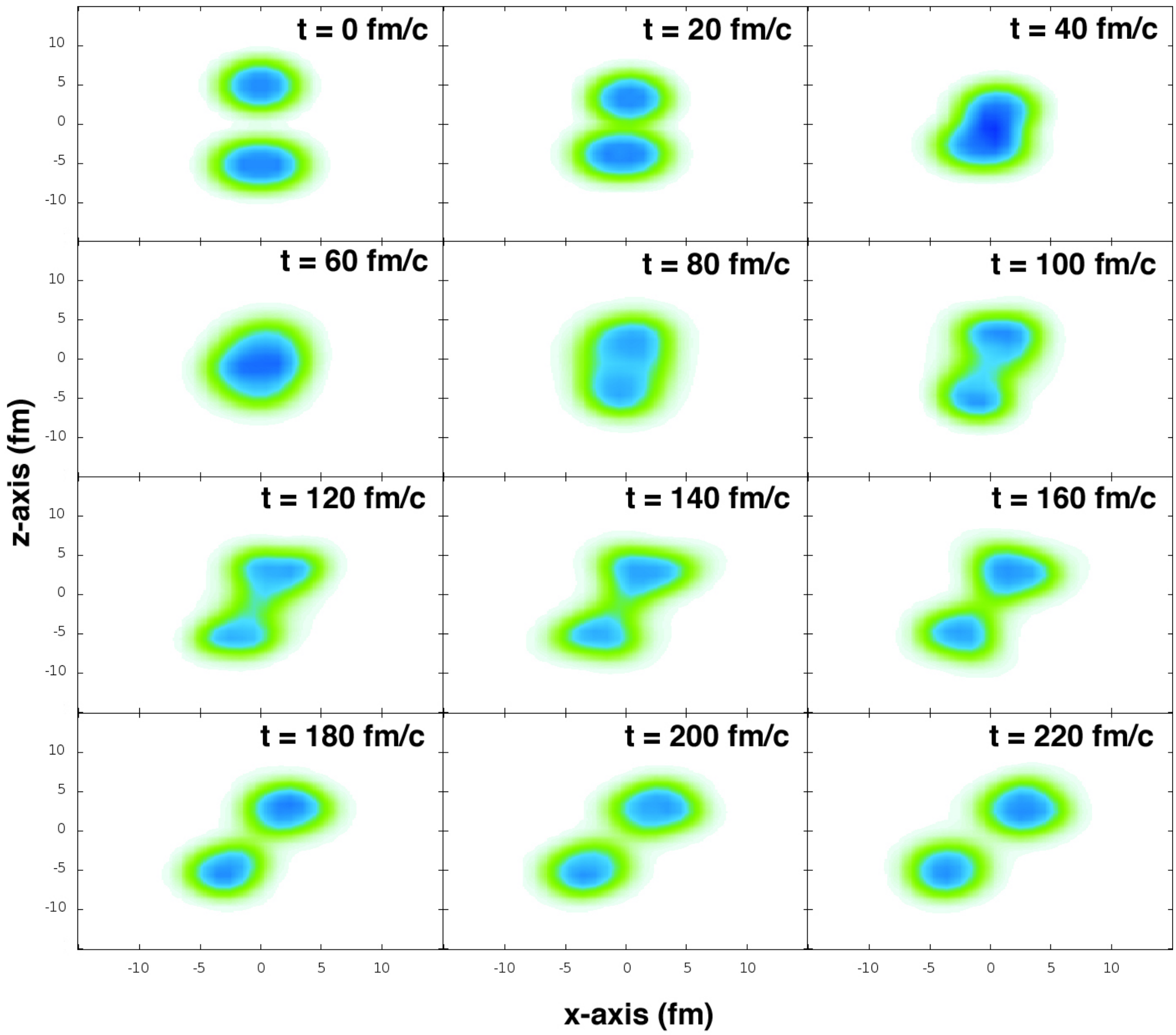

Figure 5 *Example of a Deep Inelastic Collision: ^{20}O - ^{16}O*

Again, here we have an ^{20}O nucleus colliding with an ^{16}O nucleus, under the influence of the SV-sym34 Skyrme force. In this collision, b = 2 fm, and E_{cm} = 105 MeV. The two features of note in this example are: the fact that nucleon exchange has clearly occurred (the nuclei are almost evenly sized at the end of the simulation); and the connecting neck between the two nuclei. As mentioned in the general description of deep inelastic collisions, this connecting neck is the feature by which the program evaluates whether or not the two nuclei are currently fused. Clearly, at the end of this simulation, the program would confirm that the two nuclei had separated, because there is an area of sufficiently low density between them.

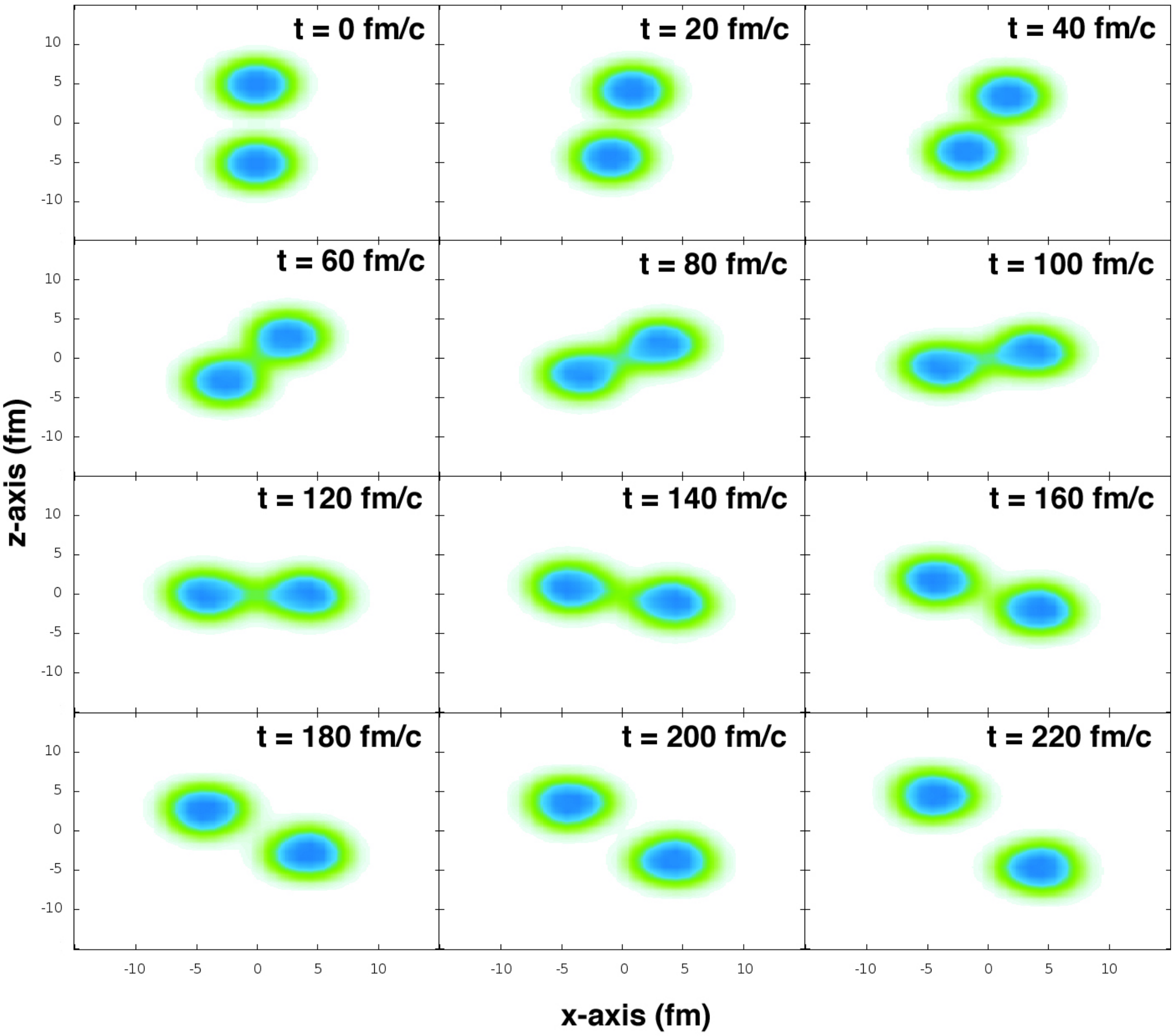

Figure 6 *Example of a Peripheral Collision: ^{16}O - ^{16}O*

In this peripheral collision, b = 6.75 fm, E_{cm} = 60 MeV, and the Skryme force being utilised is SV-bas. It can be clearly seen from these images that the two ^{16}O nuclei do make some contact during this interaction. It is entirely possible that they may have exchanged some individual nucleons, but it is impossible to determine that qualitatively using this form of output, as the nuclei are the same size before and after their interaction. NB: figures 5-7 take place over a much shorter time scale than figure 4; this is because the early stages of the reactions in figures 5-7 are the more important and physically interesting ones, whereas in figure 4 it is interesting to observe the gradual thermalisation of the system over the full 3600 iteration time scale.

Interestingly, for the collision of ^{20}O and ^{16}O, nucleon exchange could be clearly observed in the animations, as the nuclei were different in size at the beginning and and of the simulation (see fig. 5).

These animations were by far the most intuitive way to asses the outcome of each run of the program, but the scope of this project was wider, and required more information, than individual animations could provide. To find the energy and angular momentum barriers for fusion, a quantitative investigation had to be carried out.

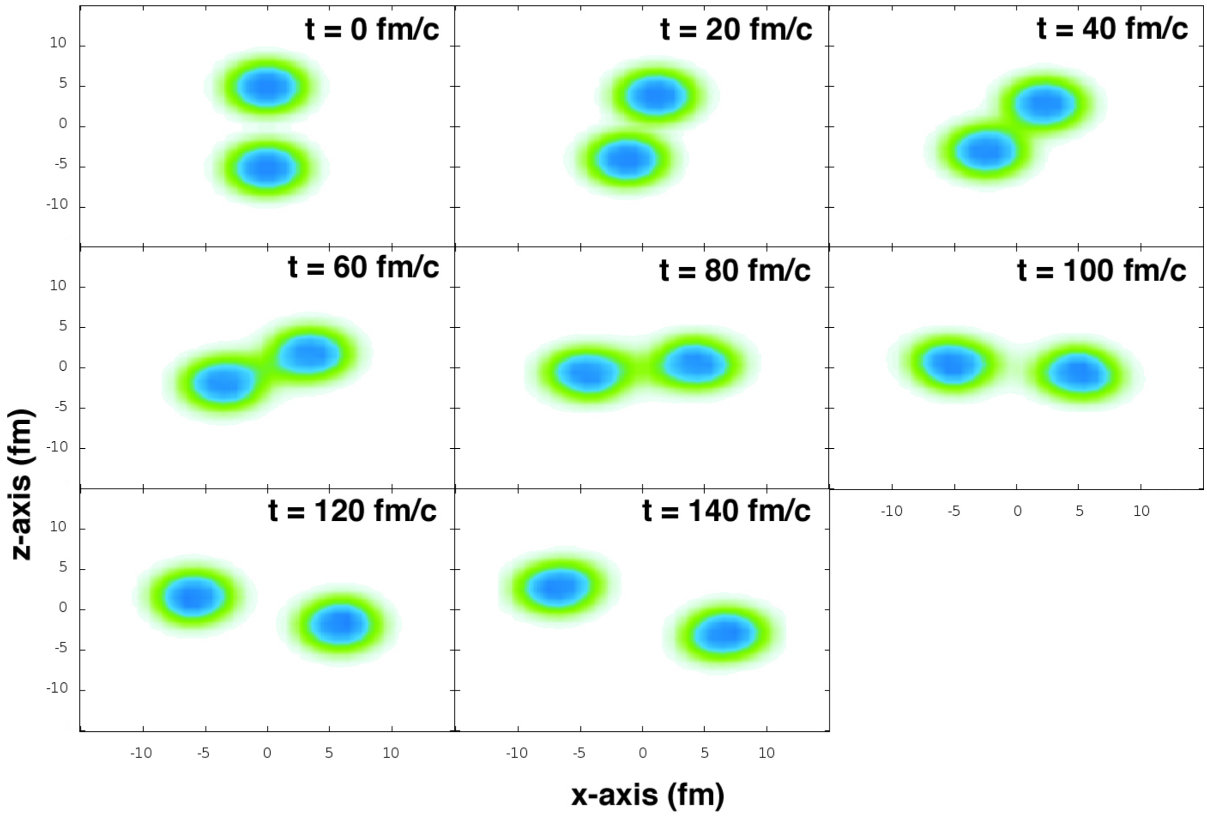

Figure 7 *Example of a Coulomb Repulsion: ^{16}O - ^{16}O*

In this interaction, b = 7 fm, E_{cm} = 105 MeV, and the Skryme force being utilised is SV-bas. Due to both the high kinetic energy of the nuclei, and the large impact parameter, this interaction is very brief. It should be mentioned that this is actually an example of a highly energetic Coulomb repulsion. Normally, at such a large impact parameter, the nuclei would not make any contact whatsoever, but due to their high kinetic energy they are able to glance past one another. They do not, however, pass close enough for any exchange interactions to occur, and therefore this is not a peripheral collision.

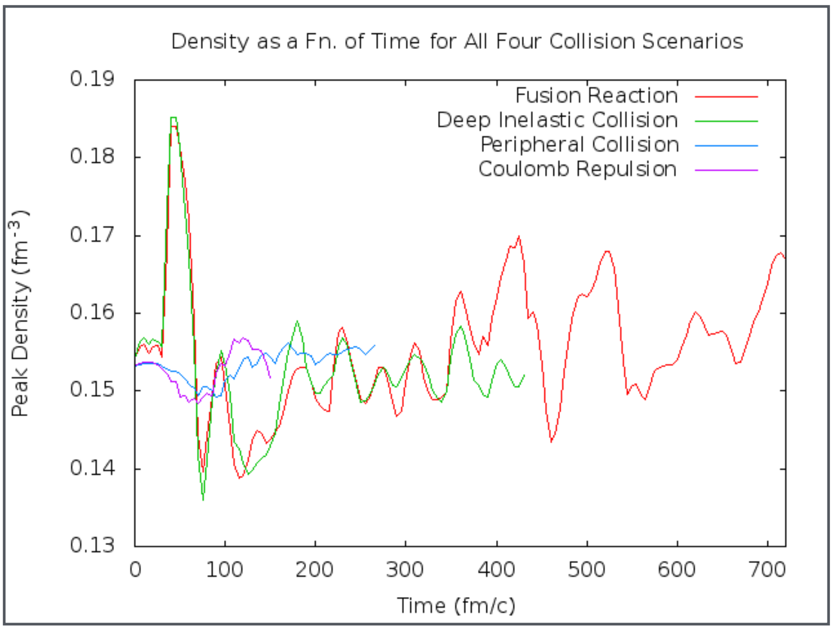

Figure 8 *A Quantitative Density/ Time Graph*

Shown here in fig. 8 is a more quantitative representation of how the density of the collision scenarios shown in figs. 4-7 evolve over time. Of note is the difference in magnitude of the time shown for the fusion reaction and the others. In comparison, the peripheral collision and Coulomb repulsion take place over much shorter time scales. The associated curves end when the two nuclei will have left the designated grid spacing.

4. The Fusion Threshold Energy

4.1 Mapping Out the Energy and Angular Momentum Window for Fusion

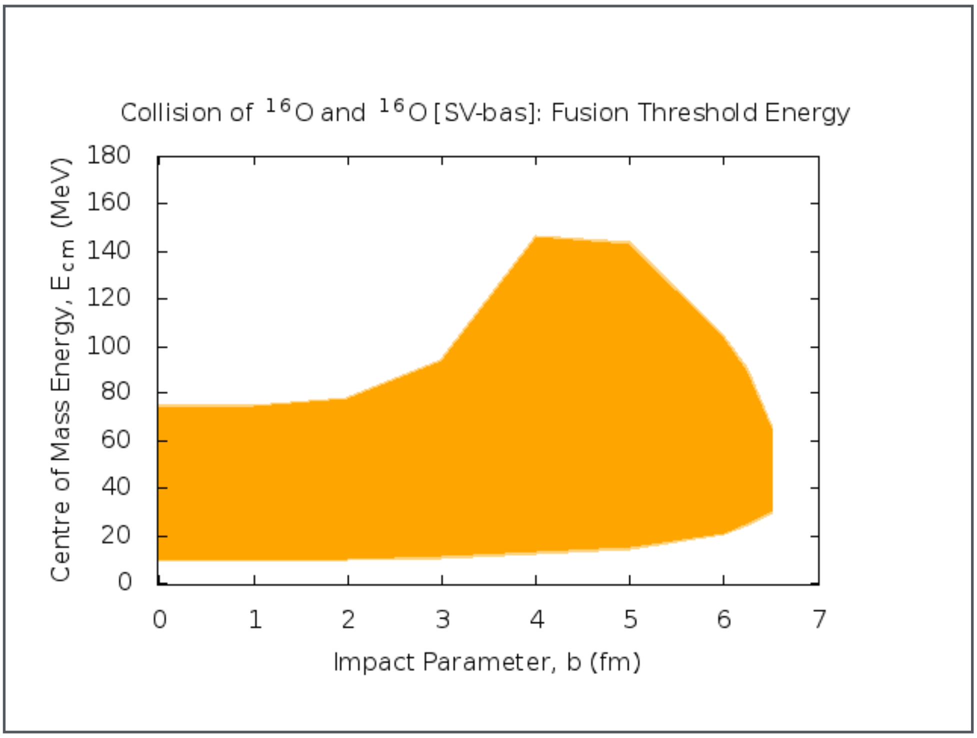

Figure 9 *FTE for two colliding ^{16}O Nuclei Using the SV-bas Skyrme Force*

Figures 9-16 show the fusion threshold energy (FTE) for their respective reactions. Figures 9, 10 and 13 were all created using the SV-bas force, which was the first Skyrme force (in a list that consisted of a total of 37 forces) that was provided with the *Sky3D* code. Figures 11, 12, and 14 were made using a different force: SV-sym34. Both of these Skyrme forces belong to the 'SV' family, so share many similar characteristics. However, they have slightly different values for the eight parameters ($x_0, x_1, x_2, x_3, t_0, t_1, t_2, t_3$) that were mentioned earlier.

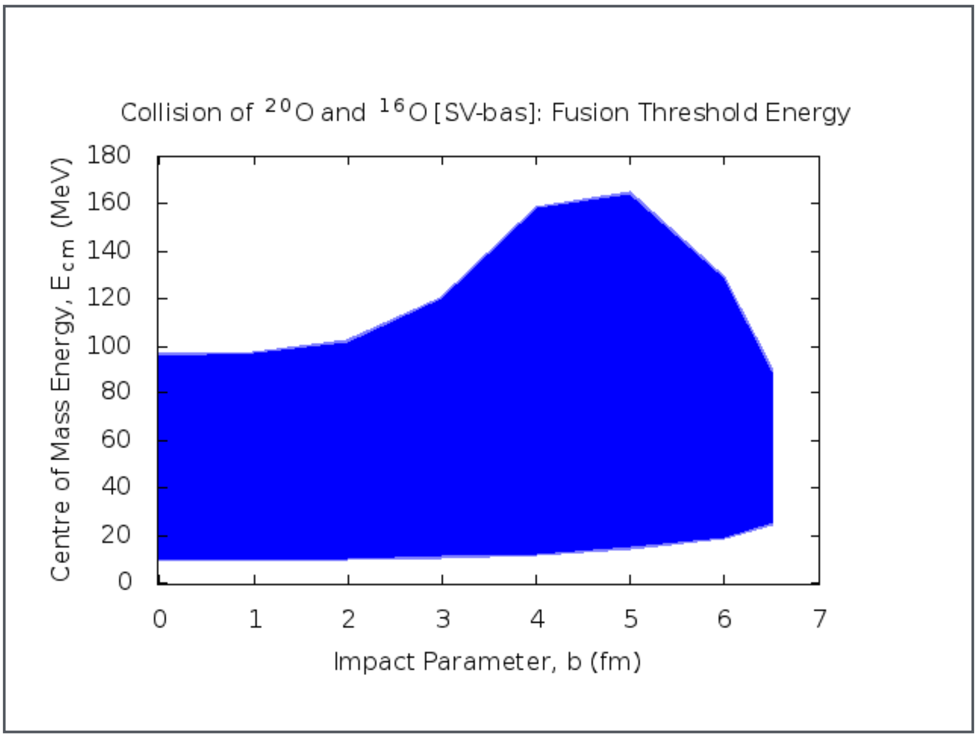

Figure 10 *FTE for ^{20}O colliding with ^{16}O Using the SV-bas Skyrme Force*

The difference between the two force models was small, but still tangible, and is shown in figure 14. Both forces followed the same profile, and had peaks in the same

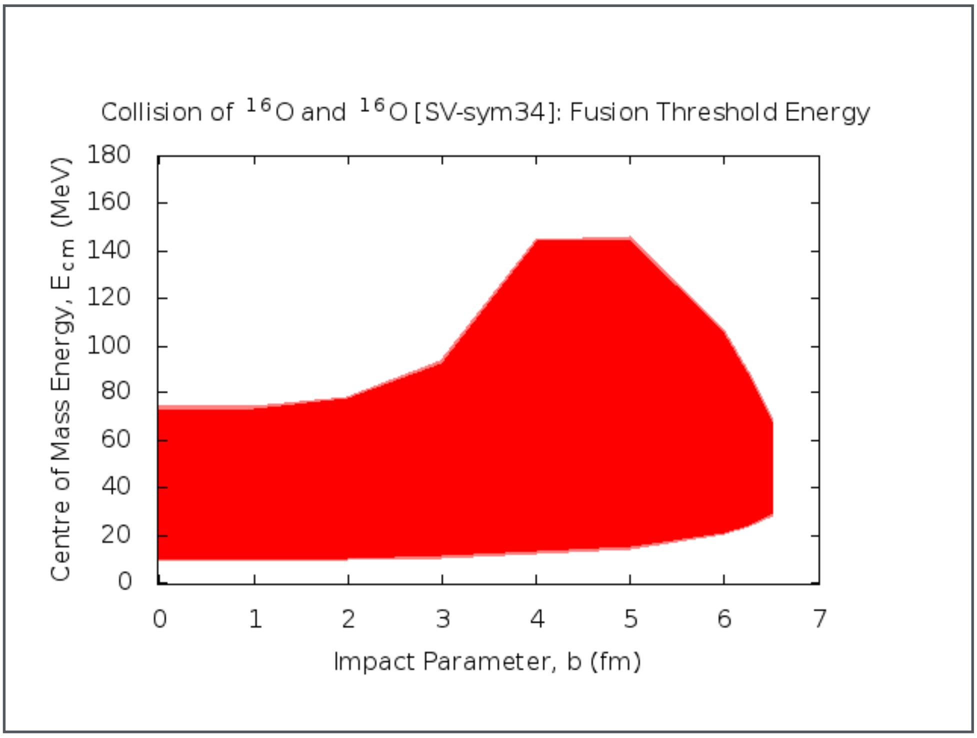

Figure 11 *FTE for two Colliding ^{16}O Nuclei Using the SV-sym34 Skyrme Force*

impact parameter range, but on average, the simulations using SV-sym34 were capable of reaching energies of between 1-3 MeV higher than that of SV-bas (see fig. 15). It must be noted at this point, that the highest resolution in energy that was attainable in the time allowed for this investigation was ±1 MeV. Two Skyrme forces from the same family were chosen because, as is evident, even a slight change in the force parameters could lead to a large change in the FTE.

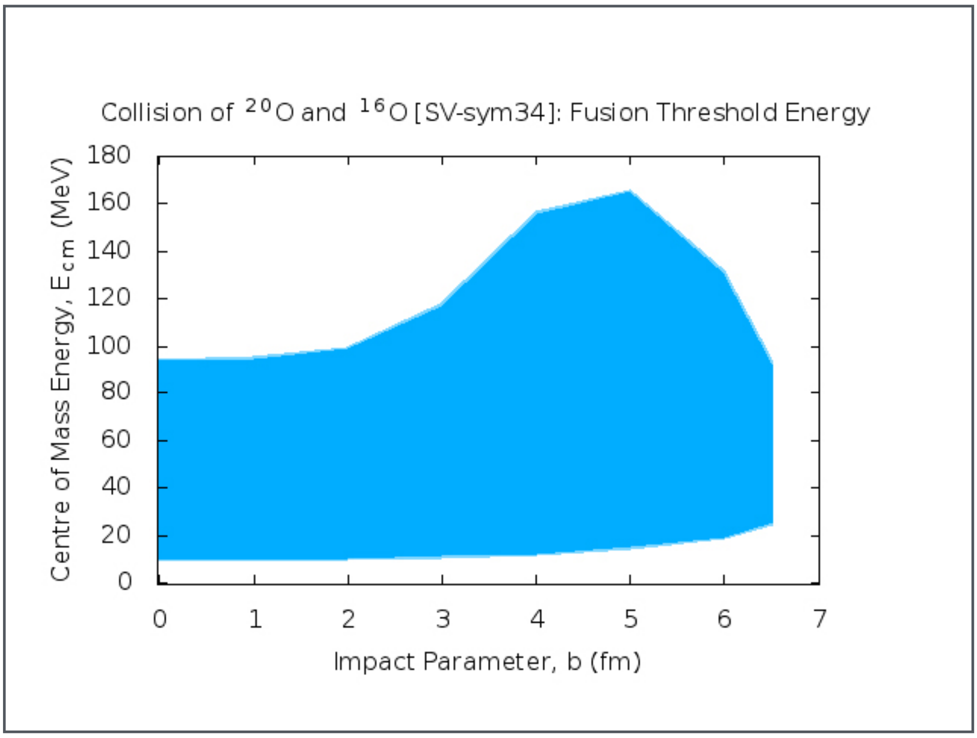

Figure 12 *FTE for ^{20}O Colliding with ^{16}O Using the SV-sym34 Skyrme Force*

Due to the numeric nature of this investigation, it was of paramount importance (in the interest of conserving time and effort) that one was able to make informed estimates as to the approximate energies at which the FTE could be found.

The shaded areas on each of these graphs denotes the energy and angular momentum range in which successful fusion is possible. Outside of this range, the two nuclei either have too much kinetic energy to reach a stable composite state, or there is too great a force of Coulomb repulsion between the nuclei for them to fuse, i.e. they cannot reach the

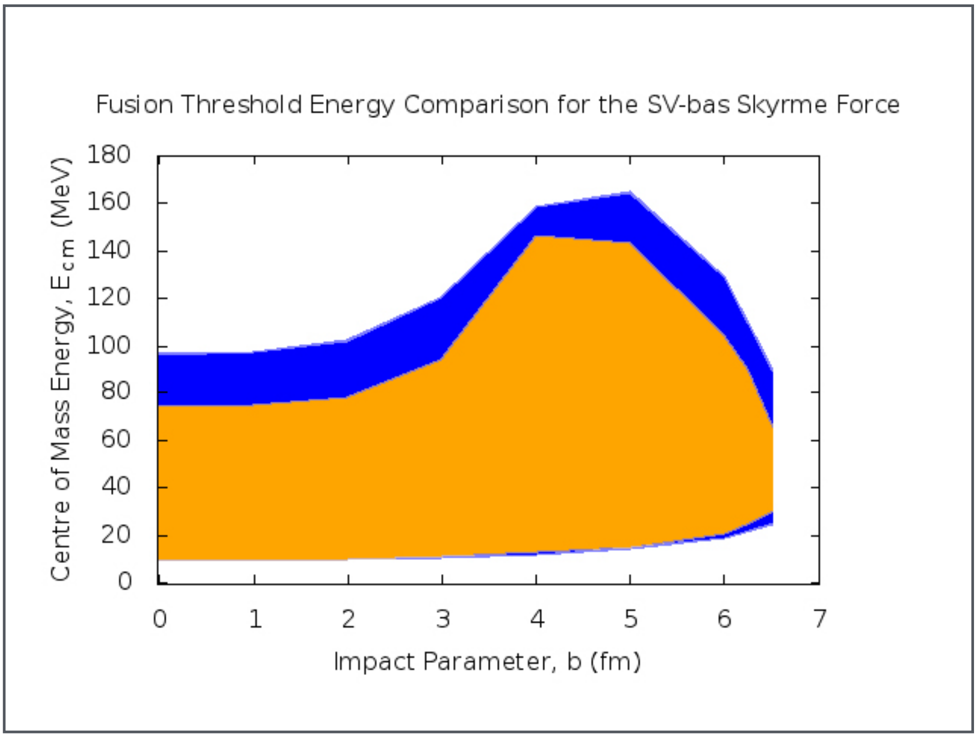

Figure 13 *Comparison of the FTEs for both SV-bas Collisions*

critical distance at which the nuclear strong force would have taken action and created a stable system.

All four reaction types showed a similar characteristic shape, consisting of a relatively flat lower boundary that increased at a greater rate at higher impact parameters, and a relatively steep upper boundary, with a clear peak between b = 4-5 fm.

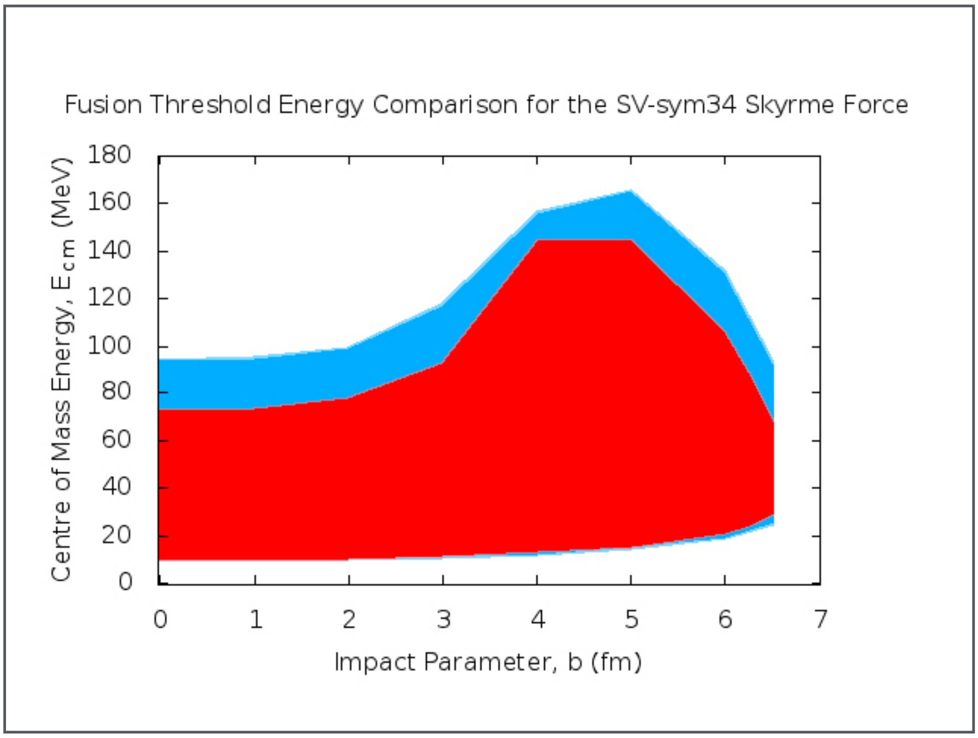

Figure 14 *Comparison of the FTEs for both SV-sym34 Collisions*

The shape of these FTE graphs is almost exactly what was expected. Fusion is possible at higher energies when the systems have larger angular momenta. This is because the energy of the system can be distributed more evenly due to the composite body's need to conserve it's angular momentum. This process of thermalisation can also be achieved through several other means, including; nucleon-nucleon collisions, energy-level excitations, and heat/ kinetic energy loss.

An interesting feature of note, is that for the collision of ^{20}O and ^{16}O, in both cases, the lower boundary for fusion is slightly lower than it is for that of two colliding ^{16}O nuclei. This is due to the sheer increase in size of the neutron rich ^{20}O nucleus. Because the only increase in mass/ volume has come from the addition of neutrons, there is no additional charge being brought into the system, and therefore the repulsive Coulomb force will be no greater than it was in the ^{16}O - ^{16}O collision. Hence fusion is more likely to occur, because the effective distance between the two nuclei is decreased due to the increase in volume provided by the four extra neutrons. It is commonly known that, assuming the nucleus is spherical (which is a key assumption of the *Sky3D* code [1]), the volume of a nucleus is directly proportional to it's mass number, *A*.

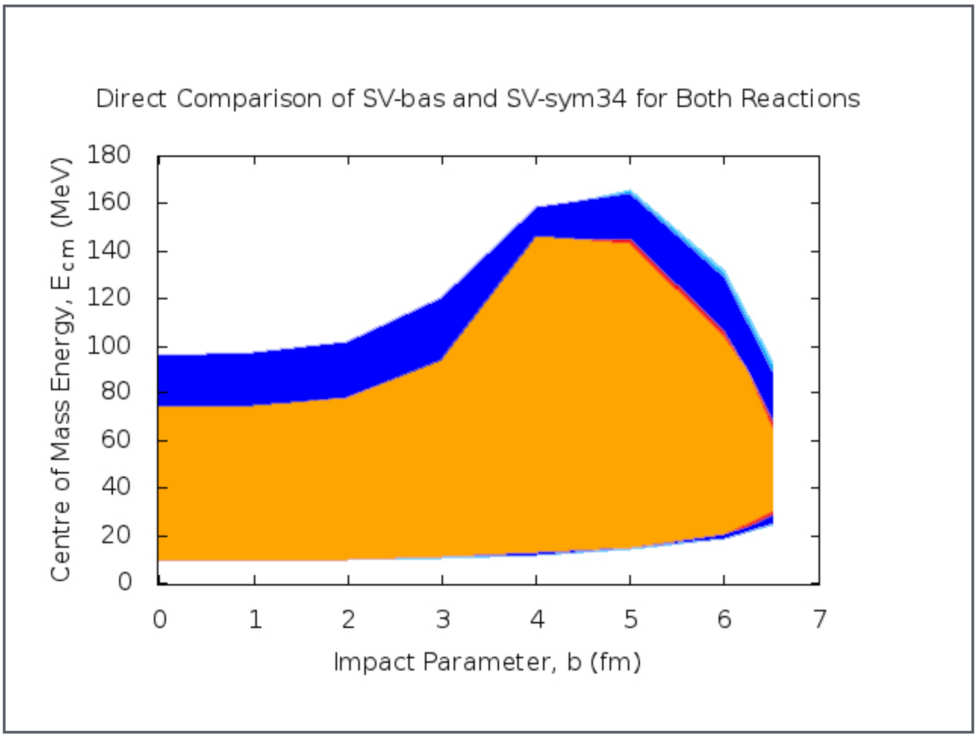

Figure 15 *Comparison of the Skyrme Forces SV-bas and SV-sym34*
It is a subtle difference, but it is still a visible one. There is very little variation between the forces at low impact parameters (*b* < 2 fm) but at higher impact parameters the difference is significant. SV-sym34 allows for higher energies at all impact parameters > 3 fm.

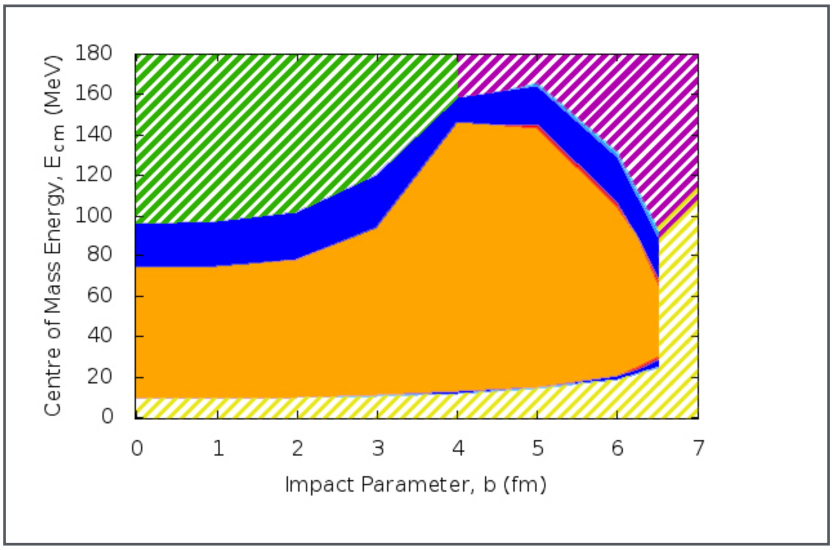

Figure 16 *An Energy/ Angular Momentum Map of the Four Collision Scenarios*

Shown here in fig. 16 is a rough guide to where on the energy/ angular momentum spectra the three other collision scenarios occur. This is by no means an exact map, but shows clearly that the individual zones are as definable as the one for fusion is.

5. Fusion Cross Section

5.1 Comparison of the TDHF Solution to Experimental Data

Fusion reaction cross sections have been researched extensively for many years. The experimental data used in fig. 17 was published in 1978 [12]. The result shown in fig. 15 is similar to that published in *Treatise on Heavy-Ion Science Volume 3: Compound System Phenomena* [3]. It shows that a cross section measured experimentally is systematically greater than that calculated using TDHF computer models.

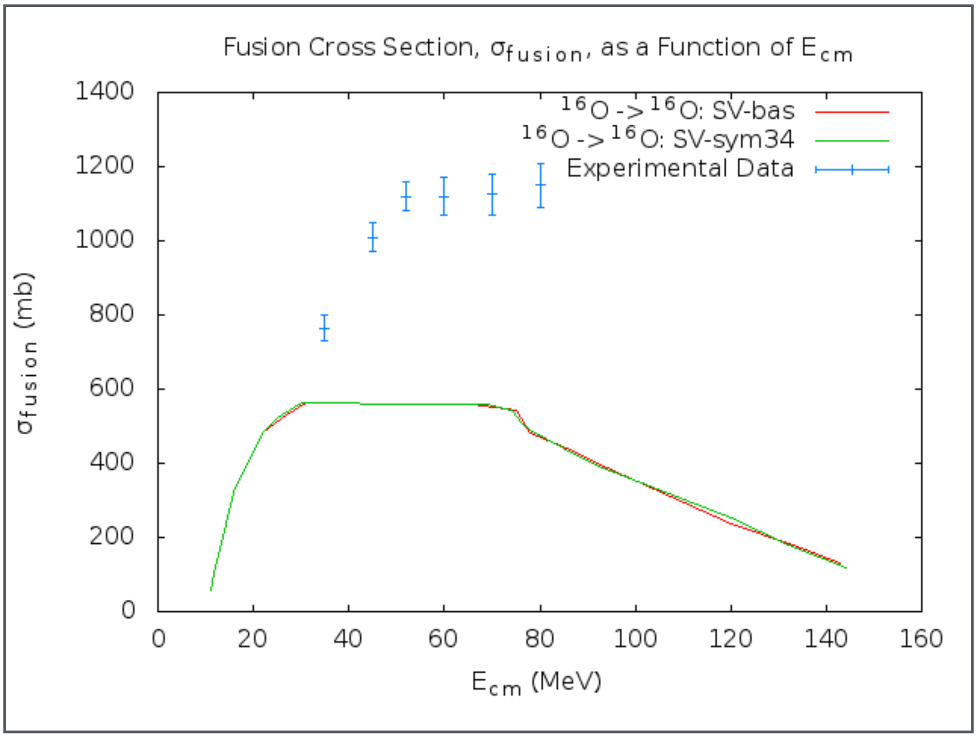

Figure 17 *Comparison of Experimental Data and TDHF Values for Fusion Cross Section*

The experimental data shown is clearly much greater than the results gained from the TDHF simulations, but it does have somewhat of a limited range. It would have been preferable to find some experimental data across the entire energy/ angular momentum spectra, as it could be that the TDHF simulations fit very well at low or high energies, just not in the mid range.

In regards to the classical, qualitative method of defining a successful fusion discussed on page 7, it was found that the “single complete rotation assumption” held up surprisingly well in these simulations. The only instances in which the system had undergone one or more complete rotations have been those where fusion was successful. This is due in part, however, to the fact that rotation only occurs at high impact parameters, and at high impact parameters the upper boundary for fusion is significantly energetic, meaning that above this boundary the two nuclei separate rapidly, i.e. before a significant angle is rotated through. The area where the most rotation occurs is on the upper boundary for fusion at high impact parameters, e.g. $4 \leq b \leq 6.5$.

Another factor to consider is the time scale of these simulations. As can be seen in fig. 4, the composite system had yet to reach a steady state of thermal equilibrium, so It cannot be conclusively said that the system did not decompose some time after that, through means of a fission or otherwise. This becomes more and more apparent at higher energies and angular momenta, as the composite nucleus is excited further and further away from its stable state.

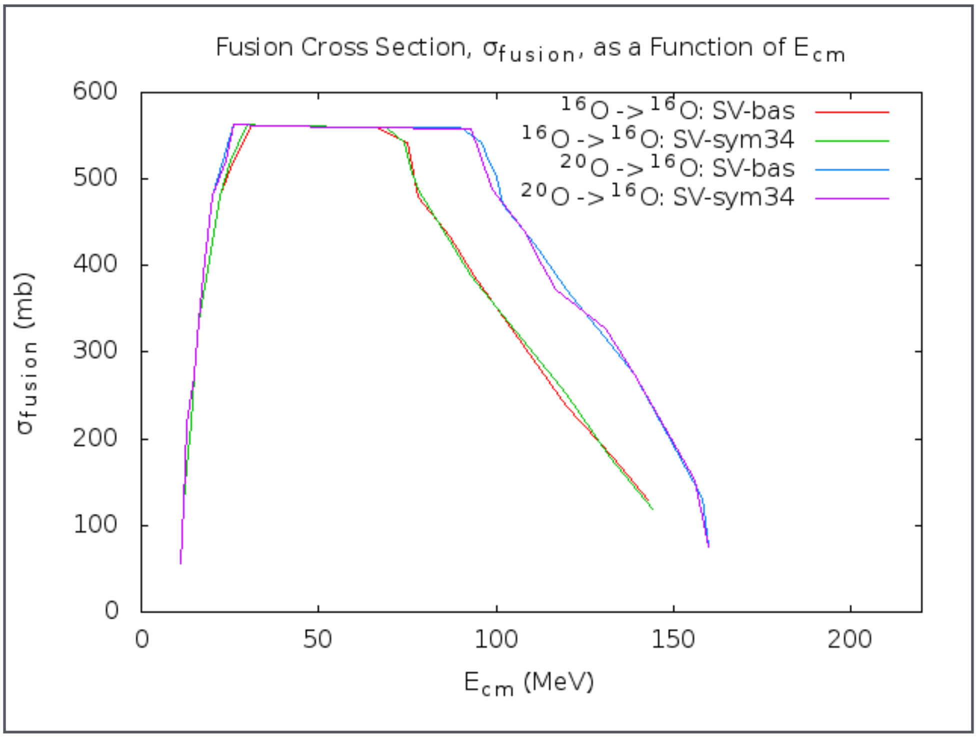

Figure 18 *A Comparison of the Fusion Cross Sections of the ^{16}O - ^{16}O Collisions and the ^{20}O - ^{16}O Collisions*

As I was not personally able to locate experimental data for any ^{20}O - ^{16}O collisions, I am only able to make comparisons between them and the smaller ^{16}O - ^{16}O collisions. It is clear still that there is a maximum cross section in the mid-range of energies, but this maximum is limited by the coulombic repulsion of the nuclei, i.e. above an impact parameter of b = 6.5 none of the nuclei are able to fuse. The fact that all four TDHF calculations follow the same pattern affirms that there is either some discrepancy in the TDHF approach, or perhaps in the way that the experimental data was collected. It must be remembered I think that these TDHF calculations are very precise in terms of time scale. In a laboratory setting there is scope for error in that some reactions may appear to be primary fusions, but instead may be secondary, i.e. a first composite nucleus may have disintegrated/ quasi-fissioned and then those lighter components may have gone on to fuse again.

6. Conclusions

To summarise the results shown in this report, I think it's been shown that the TDHF code *Sky3D* is capable of accurately modelling all the aforementioned varieties of nuclear interaction. Specifically for fusion reactions, It has been shown conclusively that at higher angular momenta the colliding nuclei can have greater individual kinetic energies (i.e. the system has a greater centre of mass energy) and still produce a stable, composite nucleus. However, if the impact parameter of the collision is too high, fusion will never occur due to the Coulombic force of repulsion between the two nuclei.

It has been shown that more massive nuclei are capable of fusing at both higher and lower kinetic energies. However, this would have been better investigated, given more time, by simulating collisions of much larger nuclei, e.g. ^{40}Ca - ^{40}Ca. The computational time required to complete a simulation of that size was unfortunately too great for the scope of this project. Generally speaking, most aspects of this project could have been vastly improved by more time. It would have been ideal to run the simulations over a much greater number of time steps to see if any of the seemingly stable composite bodies would decay over time. Another advantage of more time would have been to more accurately plot out the fusion threshold energy graphs. At present, the current resolution is ±1 MeV on the y-axis, and ±1 fm on the x-axis (with the exception of the range $6 \leq b \leq 6.5$, which had a resolution of ±0.25 fm, which was necessary to map out the right hand side of the curve). This resolution failed to show a clear peak, which although might not be completely necessary, would have been an interesting point of comparison between each of the results.

It was disappointing that I was not able to find a complete set of experimental data. It would have been interesting to see if the TDHF model was a good fit at lower energies in particular, because there was little to no difference in the lower boundary for fusion between the lighter and heavier collisions.

I would also have liked to have investigated more throughly the process, and frequency, of nucleon transfer in these reactions. *Sky3D* was capable of determining how much mass was in each half of the grid spacing at any time. It would have been interesting to map out the areas on the energy/ angular momentum spectra where the most/ fewest nucleons were transferred. I would hypothesise that the most nucleon transfer would occur at both higher energies and angular momenta.

7. References

[1] J. A. Marhun, P.-G. Reinhard, P. D. Stevenson, A. S. Umar, *The TDHF Code Sky3D*, arXiv:1310.5946, 2013.

[2] P. E. Hodgson, E. Gadioli, E. Gadioli Erba, *Introductory Nuclear Physics*, Oxford University Press, Oxford, 1997.

[3] K. T. R. Davies, K. R. S. Devi, S. E. Koonin, M. R. Strayer, *TDHF calculations of heavy–ion collisions*, in: D. A. Bromley (Ed.), *Treatise on Heavy–Ion Physics, Vol. 3 Compound System Phenomena*, Plenum Press, New York, 1985.

[4] E. B. Suckling, *Nuclear Structure and Dynamics from the Fully Unrestricted Skyrme-Hartree-Fock Model*, Department of Physics, F.E.P.S., University of Surrey, 2011.

[5] P. Bonche, B. Grammaticos, S. E. Koonin, Phys. Rev. C **17**:1700, 1978.

[6] S. E. Koonin, K. T. R. Davies, V. Maruhn-Rezwani, H. Feldmeier, S. J. Kreiger, J. W. Negele, Phys. Rev. C **15**:1359, 1977.

[7] P. Hohenberg, W. Kohn, *Inhomogeneous Electron Gas*, Phys. Rev. B **136**, 864, 1964.

[8] W. Pauli, *Über den Zusammenhang des Abschlusses der Elektronengruppen im Atom mit der Komplexstruktur der Spektren*, Z. Phys. **31**:765, 1925.

[9] Ph. Chomaz, *Collective Excitations in Nuclei*, GANIL **BP 5027**, 1997.

[10] P. A. M. Dirac, *Note on Exchange Phenomena in the Thomas Atom*, Mathematical Proceedings of the Cambridge Philosophical Society, 26, pp 376-385, 1930.

[11] M. Bender, P.-H. Heenen, and P.-G. Reinhard, *Self-Consistent Mean-Field Models for Nuclear Structure*, Rev. Mod. Phys. **75**, 121, 2003.

[12] B. Fernandez, C. Gaarde, J. S. Larsen, S. Pontoppidan and F. Videbaek, *Fusion Cross Sections for the ^{16}O - ^{16}O Reaction*, Nuclear Physics **A306**, pp 259-284, 1978.